Project Title: Enhancing the Effectiveness of Carbon Dioxide Flooding by Managing Asphaltene Precipitation

Technical Progress Report

Period Ending 03/09/2000

Principal Author: Milind D. Deo

Contract Number: DE-AC26-98BC15107

Department of Chemical and Fuels Engineering
University of Utah
Salt Lake City, UT 84112

Disclaimer:
This report was prepared an account of work sponsored by an agency of the United States Government. Neither the United States Government nor any agency thereof, nor any of their employees, makes any warranty, express or implied, or assumes any legal responsibility for the accuracy, completeness, or usefulness of any information, apparatus, product or process disclosed, or represents that its use would not infringe privately owned rights. Reference herein to any specific commercial product, process, or service by trade name, trademark, manufacturer, or otherwise does not necessarily constitute or imply its endorsement, recommendation, or favoring by the United States Government or any agency thereof. The views and opinions of authors expressed herein do not necessarily state or reflect those of the United States Government or any agency thereof.

Objectives

The project has three main objectives:

1. To determine conditions at which carbon dioxide induced precipitation occurs and to develop a thermodynamic model for the precipitation process.
2. To evaluate if kinetics of precipitation is important and to examine if precipitation can be inhibited.
3. To establish compositional variations occurring during a carbon dioxide flood and to determine if these lead to precipitation.

Summary of Work Done

Solid samples from previous thermodynamic experiments were analyzed using the Time of flight Mass Spectrometer (TOF-SIMS). Preliminary analyses indicate that signatures of asphaltenes precipitated from different oils, and at different conditions had similar "signatures". Second significant finding was that the concentrations of higher molecular weight compounds (> 800 molecular weight) were extremely small.

A secondary carbon dioxide core flood was completed. The objective of the flood was to simulate "wellbore" conditions which could be causing precipitation. The purpose of the experiment was also to verify the hypothesis that precipitation under multiple contact conditions is significantly greater than under equivalent single-contact conditions.

Analyses of kinetic experiments performed using n-alkane solvents revealed that the Scatchard-Hilderbrand Theory was reasonable in predicting the heat of mixing of alkane solvents with oil and in predicting solids precipitation from oils.

Several live oil experiments at various carbon dioxide concentrations were completed. Asphaltenes from these experiments, and pentane and heptane insolubles from different samples were analyzed using high-temperature gas chromatography (HT-GC), gas chromatography-mass spectrometry (GC-MS), time of flight secondary ion mass spectrometry (TOF-SIMS).

A polydisperse thermodynamic model of asphaltene precipitation from the oil was developed.

Temperature changes resulting due to solvent induced precipitation were modeled using ideal solution theory and kinetic parameters of precipitation were derived.

Description of the Work and Results

Asphaltene Analyses

TOF-SIMS was used on asphaltene samples from the Rangely oil field and from the asphaltenes precipitated from oil from Phillips Petroleum Compnay (a more asphaltic crude oil from southern Utah). The positive ion images from the two samples are shown in Figures 1 and 2. The intensities have been plotted at three different mass ranges in the two figures. The two signatures are very similar. Even though the relative intensities at different masses vary for the two samples, the peaks occur at identical locations. Considering that the oils are from two completely different fields and that the solids analyzed were precipitated by completely different means (one was a field sample and the other generated in our laboratories using single-contact CO_2 experiment), this finding is extraordinary. The instrument settings and analysis procedures are being examined to assess the relevance of this discovery.

A gas chromatographic signature of the field sample is shown in Figure 3. The sample reveals the occurrence of n-alkanes. Currently, an attempt is being made to reconcile the GC analyses with the TOF-SIMS results.

Kinetic Measurements

Titration experiments were performed with the Rangely crude oil and three different n-alkane solvents (n-pentane, n-hexane and n-heptane). The temperature changes of the mixtures were very closely logged with the intent of monitoring the precipitation onset. The data was analyzed using the Scatchard-Hilderbrand solution theory. The heat of

mixing curve was predicted well by the model. In the case of pentane and to a certain degree, hexane the model was reasonable in predicting in precipitation onset. The model was not good in predicting precipitation with n-heptane. All of the model equations are being evaluated rigorously to see if the technique can be applied to CO_2 induced precipitation.

Core floods

Previous core floods confirmed the compositional changes taking place in a carbon dioxide flood. The core flood performed during this period was essentially to see if these compositional changes were causing added precipitation in the core. One additional objective was to examine the behavior of fluids exiting from the core when subjected to a "wellbore" flash.

The high-pressure, core flooding experimental setup described earlier was used with some modifications. The core outlet was connected to two visual (PVT) cells. These cells were filled with carbonated brine at system conditions prior to the carbon dioxide core flood.

The sequence of operations and results were as follows. The core was mounted in a triaxial core holder and was pressurized to about 3000 psia. The pore volume of the core was recorded using volume expansion measurements. Approximately 12 different pressure cycles were used and the pore volume was averaged. The pore volume was 39 cc. The core was six inches long and was 1.5 inches in diameter for a total volume of

174 cc. The porosity of the rock was thus 22 %. The core was saturated with CO_2 at about 100 psia and was flooded with brine. After brine breakthrough, the fluids were pressurized to 2000 psia; the brine flood continued for about four PV.

The Rangely crude was introduced into the core. A total of about 4 PV of oil was sent through the core. The oil exited the core through 2 filters, a 2 micron filter and a 0.5 micron filter. This was basically to obtain a baseline for solids movement and deposition on filters without any compositional changes. The solids collected amounted to 0.1562 g or about 0.13% of the oil flowed through the filters. The core was sealed, the filters were returned online.

CO_2 was flooded through the core at 2000 psia. The oil exiting the core was filtered and collected in two high-pressure PVT cells. The PVT cells originally contained carbonated brine and thus simulated production wells. The amount of solids collected were 0.55 g for a total of 26 g of oil exiting the core. If the baseline solid value is subtracted (0.13%), this amounts to 2% solids from the oil exiting the core. The first contact precipitation amounts were all less than 1% (with the exception of one experiment, which is being repeated). Thus, the multiple contact mixture generated in the core has a tendency to precipitate twice the amount of solids as single-contact mixtures at any CO_2 concentration.

The high-pressure, oil-CO_2 mixtures collected in the PVT cells were flashed and sampled to assess the tendency of these mixtures to form solids. As a gas bubbles form and leave the flash chamber, they appeared to deposit some solid material on fittings and tubing.

This was estimated to be only about 0.06% of the oil in the chamber. The oil in both the chambers was filtered and the solids collected and weighed. The total amount of solids collected amounted to 0.11% which, given the margin of error in the measurements was close to the baseline solids amount in the oil. Thus, almost all of the solids precipitated in the multiple contact mixture were trapped at the core outlet.

Thermodynamic Experiments

A number of "live" oil experiments were conducted during the quarter. Gas containing about 5 mole% propane and 95 mole% methane was mixed with the Rangely crude to produce a an oil with a gas oil ratio of about 150 scf/STB. Three carbon dioxide induced precipitation experiments were performed with the live oil. Results from two of the experiments are summarized in Table 1. The percentage of solids precipitated in equivalent dead-oil experiments are also included in the Table for reference. Presence of gas does have significant impact on the amount of solids precipitating from the oil. Two to three times as much precipitation is likely when gas is added to carbon dioxide-oil mixtures. More experiments are underway to evaluate the effect of gas composition and the amount of gas on precipitation.

Thermodynamic Modeling

Development of a heterogeneous molecular thermodynamic model for asphaltene precipitation was completed. The oil consisted of several identifiable components and a plus fraction which was divided into a precipitating and a non precipitating component. There were essentially four adjustable parameters; ratio of the mole fraction of asphaltene to the mole fraction of the total plus fraction (β), standard deviation of the molecular weight distribution (σ) and constants a' and b', which are constants in the asphaltene and asphaltene-free crude oil interaction equation.

The model was tuned using experimental data provided by Hirschberg, et al (1984). The characterization of oil for this exercise is provided in Table 2. The experimental and model results are provided in Table 3 and the parameters employed are in Table 4. The model predicts experimental results with liquid solvents reasonably well.

The next step is to extend the model to gas induced, high-pressure precipitation. The oil composition is important in performing this analysis. Detailed Rangely crude composition and the model components and their properties are presented in Tables 5 and 6. Single-contact and multiple-contact experiments are being modeled using this composition.

Kinetic Measurements

Experiments were performed in which 10 ml of Rangely oil was placed in an insulated vessel. In the vessel is a magnetic stirrer and a thermocouple to record the temperature. The temperature is recorded as a solvent (either pentane, hexane or heptane) was added at a constant flow rate of either 1 ml/min or 2.5 ml/min. An example of the experimental results is given in Figure 4, where pentane at a flow rate of 1 ml/min is mixed with oil. It is seen that the temperature initially rises and then decreases, then finally increases. This curve appears to be the result of the superposition of two curves: 1) the initial quick rise and 2) a slowly increasing temperature profile. The initial quick rise is over by 600 sec corresponding to the point where the mole fraction solvent has reached 0.5. In this sample, some asphaltenes were precipitated by the pentane addition. Analysis of this type

of curve was performed by considering the energy of mixing, heat of mixing two liquids and heat of precipitation of the asphaltene fraction.

Consider mixing of oil with a solvent when asphaltene precipitation does not takes place. When the solvent feed temperature and the initial temperature of oil in the vessel are the same, T_0, then the overall energy balance is given by:

$$(V_o + Qt)\frac{C_v}{\boldsymbol{n}}\frac{d(T - T_o)}{dt} = E_{mix} + (V_o + Qt)\frac{\partial(\nabla H_m)}{d\Phi_1}\frac{\partial\Phi_1}{\partial t} \qquad [1]$$

As written, this equation assumes that the heat capacity, C_v, and the molar volume, ν, are constant, however, this can be changed if necessary. This assumption is reasonable, if the heat capacity and molar volume of the solvent and oil are similar or more precisely if their ratio does not vary as the solvent mole fraction is increased from zero to 0.5 and beyond. Other quantities in equation [1] are given by:

Mixing Energy per unit time = E_{mix}

Heat of mixing per unit volume, $\nabla H_m = \Phi_1(1-\Phi_1)(\delta_1 - \delta_o)^2$. [2]

where Φ_1 is the volume fraction solvent and δ is the solubility parameter for the solvent, subscript 1, and for the oil, subscript o. At any time the volume fraction of solvent is $\phi_1 = Qt/(V_o+Qt)$. The volume fraction and the mole fraction (X) are related by:

$$f_1 = \frac{\boldsymbol{n}_1 X_1}{\boldsymbol{n}_1 X_1 + \boldsymbol{n}_o X_o} \qquad [3]$$

where ν is the molar volume with subscript 1 corresponding to solvent and subscript o to oil. When oil is modeled as a true multicomponent mixture, a method to evaluate mixture molar volume and equivalent solubility parameter will have to be developed.

In equation 1, Scatchard and Hildebrand regular solution theory is used for the formulation of the heat of mixing. Upon integration the temperature difference, $\Delta T = T - T_o$, is given by:

$$\Delta T(t) = T(t) - T_o = \frac{n}{C_v}\left[\frac{\ln(1+\frac{Q\,t}{V_o})}{Q} V_o E_{mix}\right] + \frac{n}{C_v}\left[\frac{Qt}{V_o + Qt}(1 - \frac{Qt}{V_o + Qt})(d_1 - d_o)^2\right] \quad [4]$$

In this equation there are two terms; the first corresponding to mixing which slowly grows with time and the second which first increases then decreases due to the effects of the $\Phi_1(1-\Phi_1)$ term as the volume fraction of solvent increases. Figure 5 shows the separate effects of various values of E_{mix} and $(\delta_1 - \delta_o)$ on $\Delta T(t)$. Increasing the value of o increases the height of the peak observed at 10 min. At 10 minutes, the mole fraction of solvent is 0.5 corresponding to a maximum in the $\Phi_1(1-\Phi_1)$ term. Since the precipitation takes place when the mole fraction of the solvent is changing the most, i.e. in the first 10 minutes, we can use this equation for the long time effects on the temperature and by curve fitting determine the unknowns, E_{mix} and $(\delta_1 - \delta_o)^2$.

Since the maximum in the experimental data occurs at a time of approximately 100 seconds, and not 10 minutes, we can be assured that the initial quick rise is not due to solvent mixing but to precipitation of asphaltenes. Thus, we can use the best fit of equation [4] for the long time data, t>30 min, and extrapolating back to shorter times we can clearly identify the differences that must be due to precipitation. The difference between the fit and the data at short times corresponds to the enthalpy due to precipitation of asphaltenes. Figure 6 is a plot of the temperature effect of this precipitation. The point of deviation of the experimental data from the fit curve in Figure 7, indicates the

mole fraction at which asphaltene is supersaturated in the system. In this case, it is essentially immediately. Precipitation appears to stop after 10 minutes. Calculations are being continued at the present time to determine the enthalpy of precipitation (mass of asphaltenes precipitated and molecular weight of asphaltenes are necessary for this exercise).

Regular solution theory can also be used to identify the asphaltene solubility, $X_{a,eq}$.

$$
\begin{aligned}
-RT \ln X_{a,eq} &= \Delta H_{F,a} + \nu_a \phi_s^2 (\delta_s - \delta_a)^2 \\
&= \Delta H_{F,a} + \nu_a \left(\frac{\nu_1 X_1 + \nu_o X_o}{\nu_1 X_1 + \nu_o X_o + \nu_a X_a}\right)^2 ((\delta_1 X_1 + \delta_o X_o + \delta_a X_a) - \delta_a)^2
\end{aligned}
\quad [3]
$$

where R is the gas constant, T is the temperature, $\Delta H_{F,a}$ is the heat of fusion of asphaltene at a reference temperature ,T_R, ν_a is the molar volume of asphaltene, δ_a is the solubility parameter of asphaltene, ϕ_s is the volume fraction of the solvent system (oil plus solvent at any time) and δ_s is the solubility of the solvent system. The heat of fusion for asphaltene can be measured by differential scanning calorimetry of the precipitated solid. As the volume fraction of solvent (subscript, 1) is increased the volume fraction of the system approaches 1.0 and the value of the solubility parameter decreases to a value near that of the solvent. The result of both of these effects is to decrease the solubility of asphaltene as solvent is added as shown in Figure 7. Also shown is an assumed concentration of asphaltene. Initially the solution is undersaturated. At the intersection of the two curves in Figure 7, the solution is saturated. At higher mole fractions of solvent,

X_1, the solution is supersaturated. The supersaturation ratio, Xa/Xeq, is the driving force for precipitation.

References:

Hirschberg, A., deJong, L. N. L., Schipper, B. A. and Meijer, J. G., 1984, Influence of Temperature and Pressure on Asphaltene Flocculation, Society of Petroleum Engineers Journal, June 1984, 283-293.

Table 1: Comparison of asphaltenes precipitated (wt% of the oil) when using live and dead Rangely crude oil. The GOR was 150 scf/STB and the gas contained 95% methane and 5% propane.

CO_2 Mole %	50	60
Dead oil	0.2	0.8
Live oil	1.7	3.8

Table 2: Composition of the crude oil used in tuning the thermodynamic model. The composition was given by Hirschberg, et al. (1984)

Composition	(mol%)
C1	0.10
C2	0.48
C3	2.05
iC4	0.88
nC4	3.16
iC5	1.93
nC5	2.58
C6	4.32
C7+	84.50
Average MW of tank oil	221.50
Specific gravity of tank oil	0.873
Average density of asphaltene, g/cm^3	1.2

Table 3: Comparison of the experimental amounts with model predictions.

Solvent	Dilution Ratio (cm^3 solvent/g tank oil)	Exp. (wt %)	Model, (wt %)
C6	0.0	---------	0.0032
	1.0	---------	0.0039
	2.0	---------	0.0043
	3.0	---------	0.0070
	4.0	---------	0.5732
	5.0	---------	2.0694
	10.0	---------	2.5242
	20.0	---------	2.8455
	50.0	---------	2.8549
C7	0.0	---------	0.0023
	1.0	---------	0.0019
	2.0	---------	0.0066
	3.0	---------	0.1622
	4.0	---------	1.2642
	5.0	1.53	1.5262
	10.0	1.82	1.8590
	20.0	1.89	1.8609
	50.0	1.87	1.8628
C10	0.0	---------	0.0026
	1.0	---------	0.0031
	2.0	---------	0.0351
	3.0	---------	0.6981
	4.0	---------	1.1736
	5.0	1.34	1.3203
	10.0	1.45	1.4918
	20.0	1.50	1.4740
	50.0	---------	1.8811

-------- data not available

Table 4: Optimized model parameters

Solvent	β	σ	a'	b'
nC5	0.00668	167.5	0.270	-0.00247
C6	0.004965	146.25	0.2565	-0.00206
C7	0.00325	125.0	0.243	-0.00165
C10	0.00325	132.0	0.2225	-0.00115

Table 5: Detailed Rangely crude composition as measured by gas chromatography

Component	Weight %	Component	Weight %
C5	2.791435	C34	1.246557
C6	2.797687	C35	1.241887
C7	1.718041	C36	1.085021
C8	2.700792	C37	0.920742
C9	4.148689	C38	0.989896
C10	3.762076	C39	0.869194
C11	4.495995	C40	0.765496
C12	3.691702	C41	0.696806
C13	3.895433	C42	0.681447
C14	4.152392	C43	0.581452
C15	4.072598	C44	0.610525
C16	3.347929	C45	0.597152
C17	3.679020	C46	0.574754
C18	2.566236	C47	0.500537
C19	3.310149	C48	0.503767
C20	2.840317	C49	0.495502
C21	2.749553	C50	0.455431
C22	2.573762	C51	0.425555
C23	2.509332	C52	0.410303
C24	2.084314	C53	0.402739
C25	2.348433	C54	0.353844
C26	1.972203	C55	0.383281
C27	1.956050	C56	0.350282
C28	1.866888	C57	0.344287
C29	1.943955	C58	0.302389
C30	1.603736	C59	0.335875
C31	1.519809	C60	0.277878
C32	1.462037	C60+	3.748586
C33	1.288221		

Table 6: Lumped components and equations of state parameters for the Rangely crude oil.

Pseudo-Component	Mol %	MW	Pc, atm	Tc, K	ω
FC6	18.2890	81.369	32.6097	496.984	0.26963
FC9	23.0875	124.147	26.4059	604.142	0.40552
FC13	19.7670	174.360	20.5644	681.250	0.55902
FC17	13.9581	238.085	16.3045	749.600	0.72765
FC22	9.5662	303.228	13.1965	806.019	0.88804
FC29	7.5221	400.210	10.8626	862.012	1.03476
FC38	5.6119	524.146	9.4314	912.732	1.14466
FC48	2.1928	666.512	8.2688	964.174	1.25311

δ_{ij}	FC6	FC9	FC13	FC17	FC22	FC29	FC38	FC48
FC6	0.00000							
FC9	0.00237	0.00000						
FC13	0.00817	0.00176	0.00000					
FC17	0.01595	0.00611	0.00133	0.00000				
FC22	0.02411	0.01156	0.00435	0.00088	0.00000			
FC29	0.03105	0.01659	0.00765	0.00262	0.00047	0.00000		
FC38	0.03798	0.02185	0.01138	0.00498	0.00168	0.00038	0.00000	
FC48	0.04465	0.02708	0.01529	0.00769	0.00339	0.00135	0.00030	0.00000

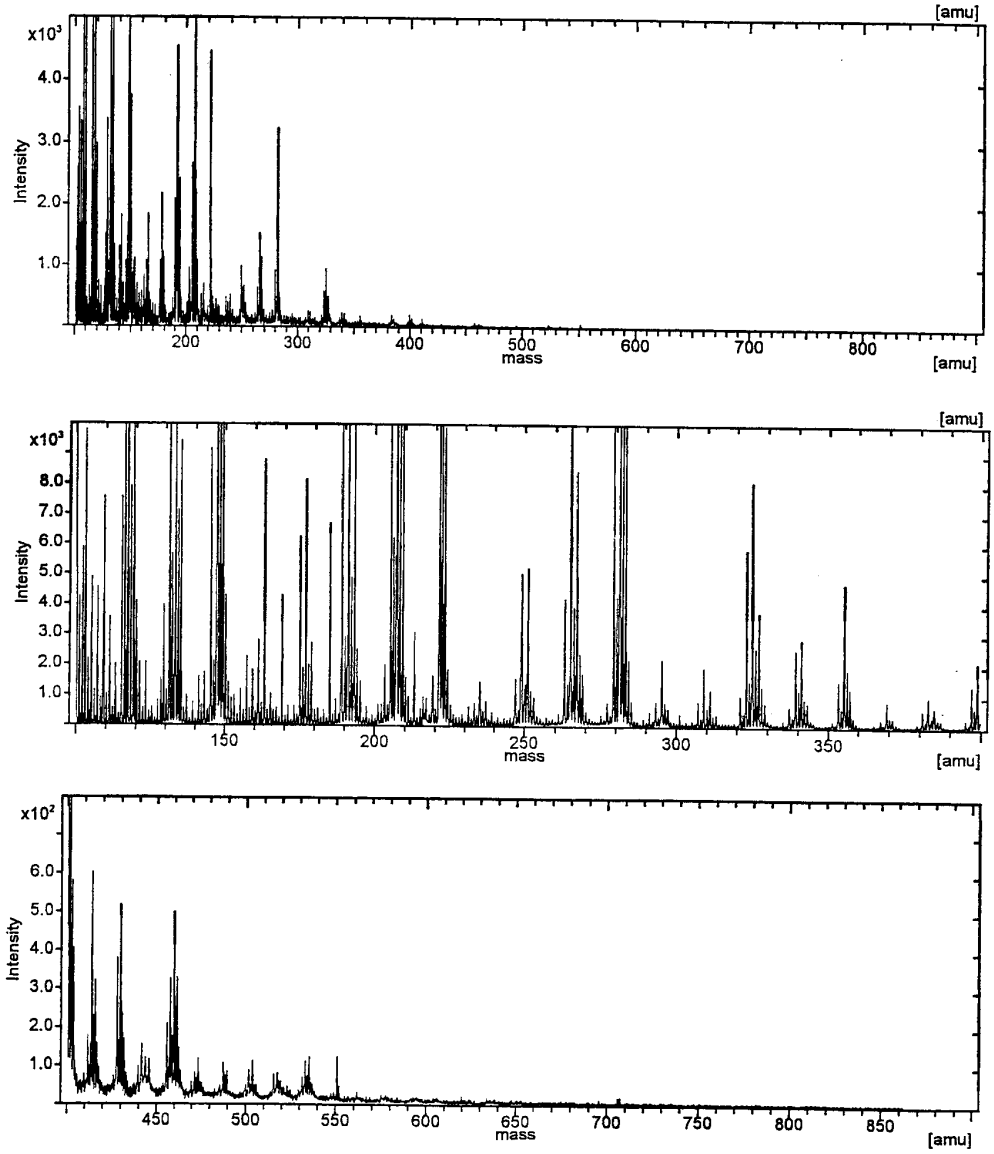

Figure 1: A positive ion TOF-SIMS(Time of Flight Mass Spectrometer) image of the asphaltenes from the field.

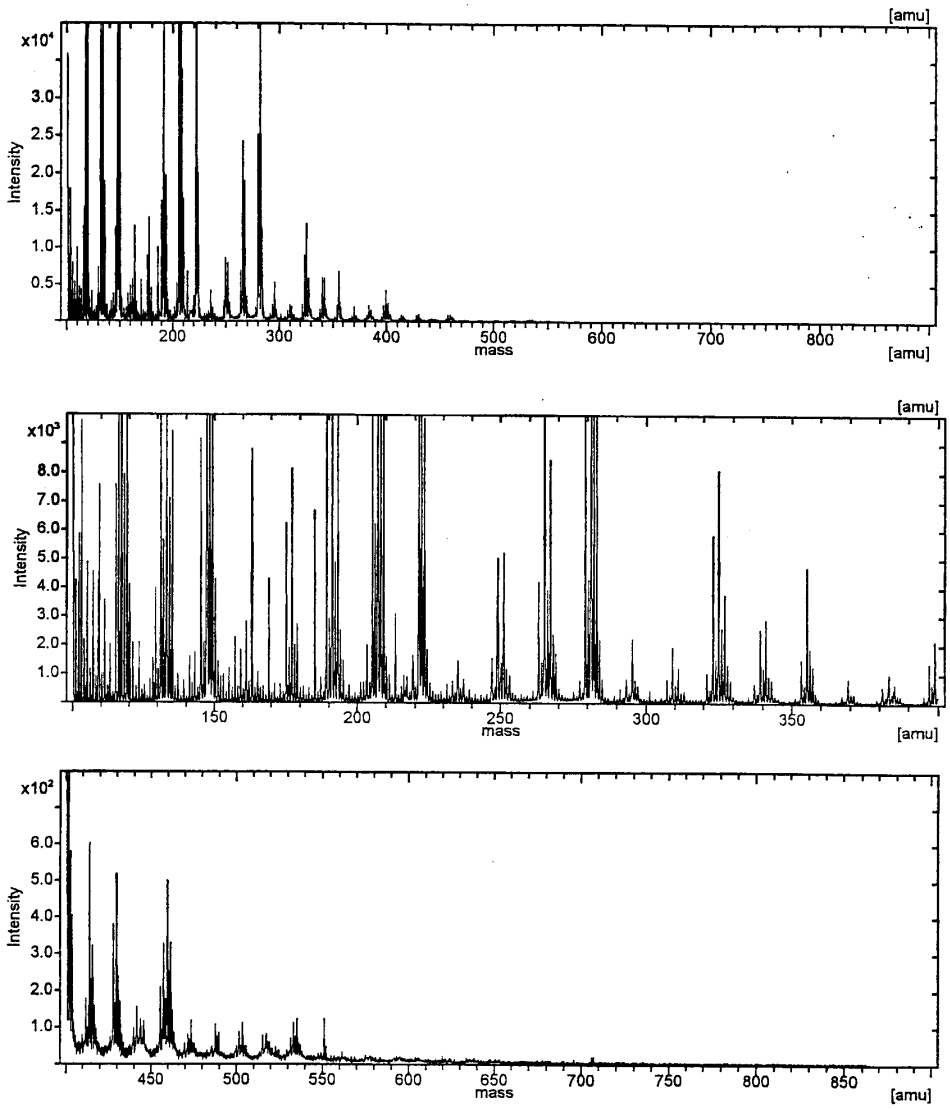

Figure 2: A positive ion TOF-SIMS (Time of Flight Mass Spectrometer) image of the solids obtained by contacting 50 mole% Phillips crude oil (oil from southern Utah) with 50% CO_2.

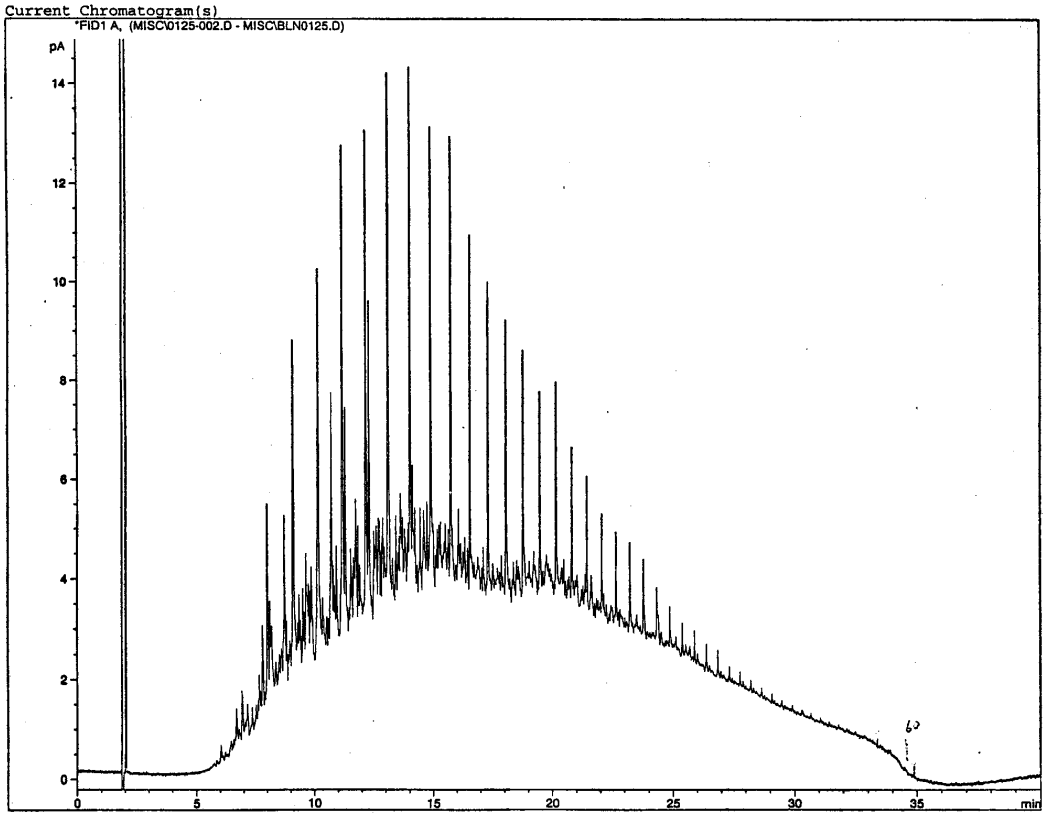

Figure 3: A high-temperature GC-FID (Gas Chromatography with Flame Ionization Detector) chromatogram of field (Rangely) asphaltenes.

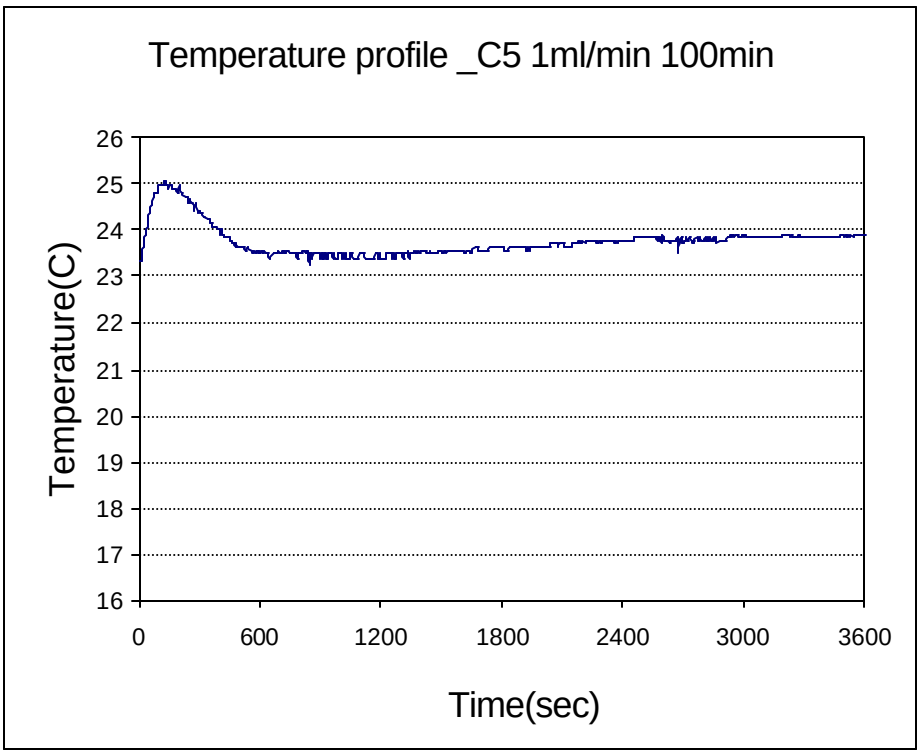

Figure 4: Temperature observation due to mixing of pentane at a flow rate of 1 ml/min into 10 ml of Rangely crude.

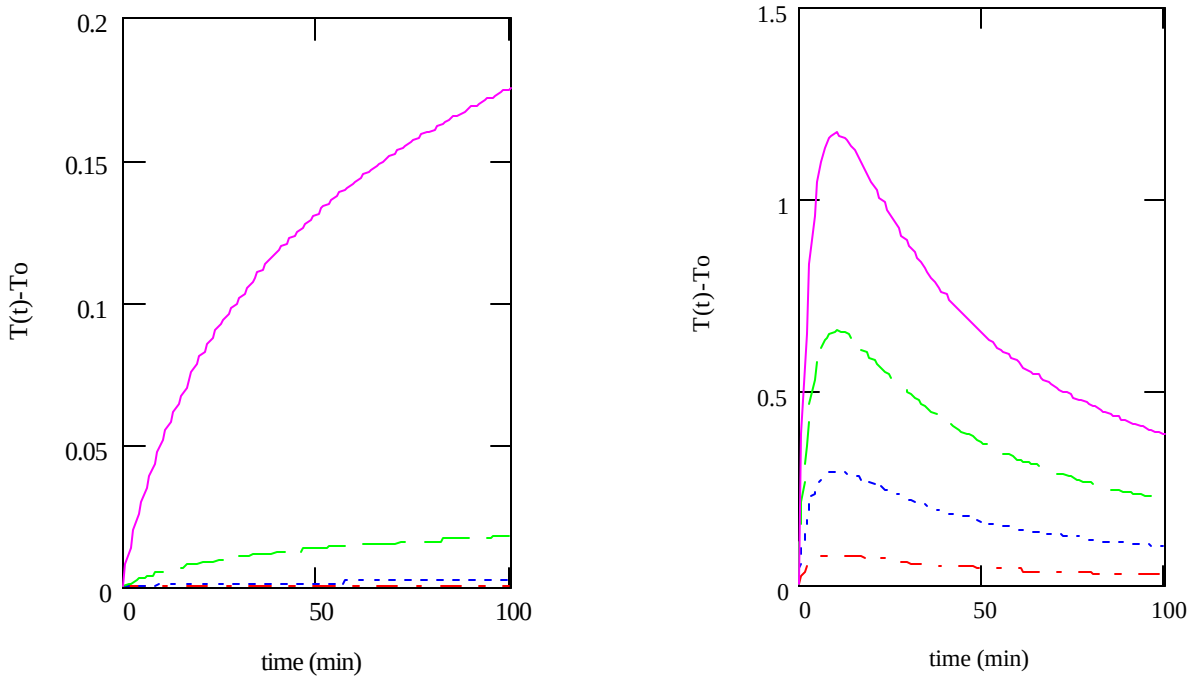

Figure 5: Effect of E_{mix} and $(\delta_1 - \delta_o)$ on $\Delta T(t)$ (°C). (a) Effect of various values of $(\delta_1 - \delta_o)$ on $\Delta T(t)$ assuming E_{mix} is zero, for curves from bottom to top $(\delta_1 - \delta_o)$ = 7.3, 7.5, 7.7, 7.9, (b) Effect of various values of E_{mix} on $\Delta T(t)$ assuming $(\delta_1 - \delta_o)$ is zero, for curves from bottom to top E_{mix} = 1 0.1,0.01, 0.001 cal/L*min. In both plots it is assumed that the molar volume and the heat capacity of the mixture do not change.

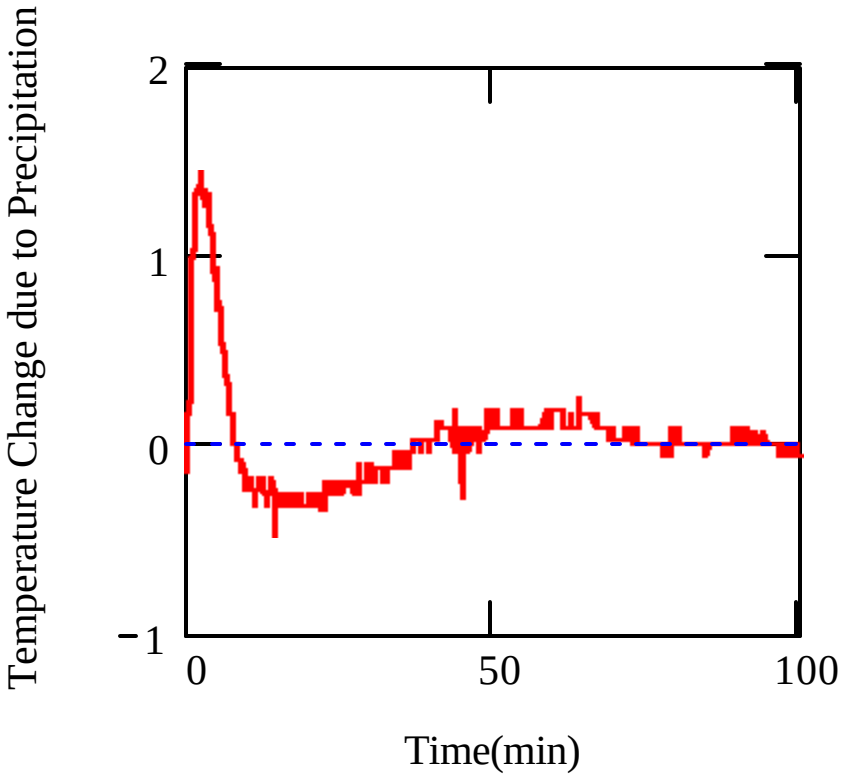

Figure 6: Difference in the experimental and curve fit of long time data identifying the temperature change due to the enthalpy of asphaltene precipitation.

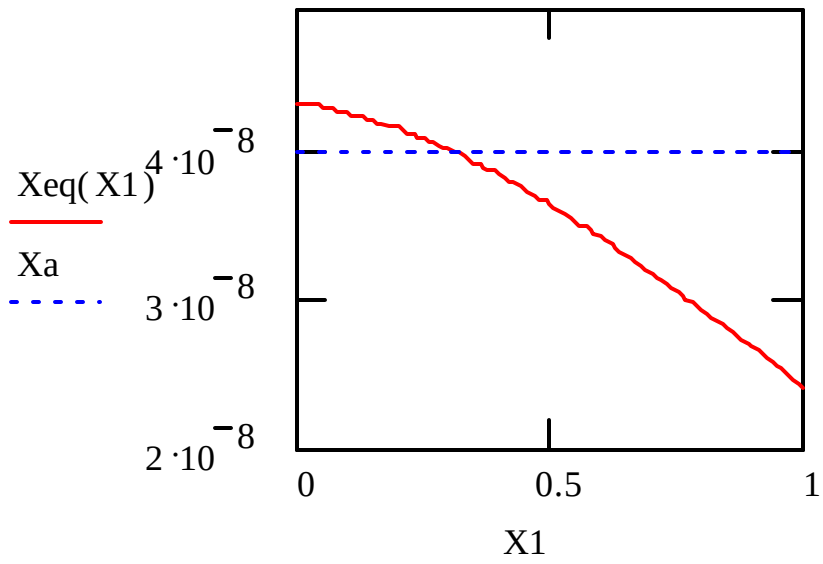

Figure 7: Solubility of asphaltene, Xeq, (solid line) and asphaltene, Xa, (dashed line), in solution assumed to be $4x10^{-8}$ as the solvent mole fraction, X1 is increased. Depending upon the amount of asphaltene in the oil, the point at which the solution is saturated will change. The saturation point is the intersection of the two curves.